# Introduction to Organic Thin Film Transistors and Design of n-Channel Organic Semiconductors

Christopher R. Newman,[‡] C. Daniel Frisbie,*[,‡] Demetrio A. da Silva Filho,[§] Jean-Luc Brédas,[§] Paul C. Ewbank,[†] and Kent R. Mann[†]

*Departments of Chemistry and of Chemical Engineering and Materials Science, University of Minnesota, Minneapolis, Minnesota 55455, and School of Chemistry and Biochemistry, Georgia Institute of Technology, Atlanta, Georgia 30332*

*Received April 14, 2004. Revised Manuscript Received June 23, 2004*

The development of new organic semiconductors with improved performance in organic thin film transistors (OTFTs) is a major challenge for materials chemists. There is a particular need to develop air-stable n-channel (electron-conducting) organic semiconductors with performance comparable to that of p-channel (hole-conducting) materials, for organic electronics to realize the benefits of complementary circuit design, i.e., the ability to switch transistors with either positive or negative gate voltages. There have been significant advancements in the past five years. In terms of standard OTFT metrics such as the field effect mobility ($\mu_{FET}$) and on-to-off current ratio ($I_{ON}/I_{OFF}$), n-channel OTFTs have achieved performance comparable both to that of n-channel amorphous silicon TFTs and to that of the best reported p-channel (hole-conducting) OTFTs; however, issues of device stability linger. This review provides a detailed introduction to OTFTs, summarizes recent progress in the development of new n-channel organic semiconductors, and discusses the critical properties that any prospective n-channel material must have. Methods important to semiconductor design such as electronic structure calculations and synthetic structural modifications are highlighted in a case study of the development of a new n-channel material based on a terthiophene modified with electron-withdrawing groups. The review concludes with a discussion of directions for future work in this area.

## 1. Introduction

Over the past 10 years there has been remarkable progress in the development of thin film transistors (TFTs) based on organic semiconductors. In terms of the key figures of merit, namely, the on-to-off current ratio ($I_{ON}/I_{OFF}$), the field effect mobility ($\mu_{FET}$), and the threshold voltage ($V_T$), the performance of the best organic TFTs now rivals that of commercial amorphous silicon TFTs, which are commonly employed as the pixel switching elements in active matrix flat panel displays. An important advantage of organic semiconductors vis-à-vis amorphous silicon is that they can be deposited onto substrates at low temperatures, meaning they are compatible with flexible plastic substrates.[1,2] A number of industrial laboratories are working hard to develop low-cost, large-area plastic electronics employing transistors and diodes based on organic semiconductors. The good performance of organic TFTs (OTFTs) makes it more likely that these efforts will succeed. As noted by Dimitrakopoulos and Malenfant in their 2002 review,[3] industrial emphasis is shifting away from organic semiconductor testing and more toward manufacturing process development.

From a materials science perspective, there remain a number of important unanswered questions concerning the performance of organic semiconductors in OTFTs.[4] For example, transistors based on polycrystalline films of pentacene, a fused ring oligomer, set the benchmark for OTFT performance, routinely displaying values of $\mu_{FET}$ in excess of 1 $cm^2\ V^{-1}\ s^{-1}$, $I_{ON}/I_{OFF} > 10^8$, and $V_T$ near 0 V.[5] It is not perfectly clear how these impressive electrical characteristics depend in detail on the crystal structure and morphology of pentacene films; TFTs based on polycrystalline films of many other organic semiconductors do not have comparable transport characteristics. Indeed, it is reasonable to ask why pentacene TFTs appear so far to be unique in their combination of exceptional transport properties. Basic understanding of structure−property relationships is essential for answering this question and a host of others including the following: How high can carrier mobilities be in films of crystalline organic semiconductors? Can good mobilities be obtained in solution-processable films that are only partially crystalline? What are the structural and electronic factors that facilitate or impede transport in organic semiconductor films? Are there particular molecular structures and crystal packing motifs that are especially favorable for transport? What is the role of grain boundaries? These unanswered questions reflect a significant gap in basic knowledge of structure−property relationships on all length scales in organic semiconductors. Perhaps the most significant point is that this knowledge gap

* To whom correspondence should be addressed at the Department of Chemical Engineering and Materials Science, University of Minnesota. E-mail: frisbie@cems.umn.edu.
[†] Department of Chemistry, University of Minnesota.
[‡] Department of Chemical Engineering and Materials Science, University of Minnesota.
[§] Georgia Institute of Technology.

10.1021/cm049391x CCC: $27.50 
Published on Web 08/31/2004

impedes rational efforts to design organic semiconductors with further enhancements in electrical performance.

A particular design need is in the area of n-channel (also commonly referred to as "n-type") organic semiconductors. As described in the next section, TFTs based on n-channel semiconductors conduct electrons and achieve their high conductivity "on" state with *positive* gate voltages, whereas most OTFTs (e.g., pentacene TFTs) are p-channel devices (i.e., they conduct holes) and turn on with *negative* gate voltages. The motivation for seeking good n-channel OTFTs is that they enable complementary circuit design. Electrical engineers are proficient at developing low-power complementary circuits that utilize both positive and negative gate voltages to turn transistors on and off. The lower power requirement of complementary circuits is an attractive feature for many potential applications for plastic electronics, such as radio frequency identification (RFID[6]) tags, in which the organic circuit must be energized by a local radio frequency (rf) field. Consequently, the development of good n-channel OTFTs with performance comparable to that of pentacene TFTs is a major goal for organic electronics.

Historically there have been more examples of good p-channel materials than n-channel materials for OTFTs. In the past five years there has been increased attention to n-channel materials, but early efforts can be traced back to the mid-1990s. Very recently, electron mobilities near 1 $cm^2 V^{-1} s^{-1}$ have been achieved in several organic semiconductors, which is on par with hole mobilities in pentacene films. However, there is currently no n-channel analogue for pentacene, i.e., an n-channel organic semiconductor that is clearly superior to all others in terms of overall performance. This situation may change soon given the intense research in this field, and progress on the vexing issue of air stability to be discussed later.

In this paper we review recent progress in the design of good n-channel semiconductors for OTFTs and specify the key requirements that these materials must satisfy to be practical. Our review complements the previously mentioned review by Dimitrakopoulos and Malenfant, who summarized p-channel and n-channel OTFT development efforts up to the summer of 2001. Specifically, we include developments that have occurred in the past two and a half years (e.g., more new n-channel materials, higher reported mobilities, and the observation of ambipolar (electron and hole) transport), and we also present a case study that summarizes our experiences in trying to develop a successful n-channel material, which we think is illustrative of the challenges and opportunities that researchers face in this area. An important theme that we emphasize is the role that electronic structure calculations can play in identifying and designing promising n-channel semiconductor candidates.

## 2. OTFT Geometry and Operation

Parts a and b of Figure 1 show cross-sections of top-contact and bottom-contact transistor geometries that are most commonly used for OTFTs. In both cases, an organic semiconductor film is deposited on a gate/insulator substrate and is contacted with metallic source and drain electrodes. In the top-contact case, Figure 1a, the organic film is deposited first, followed by the metal electrodes. In the bottom-contact case, Figure 1b, this deposition sequence is reversed. Usually, the gate/insulator assembly consists of a metal or doped semiconductor gate electrode coated with an insulating oxide (typically 200−400 nm thick), though polymeric insulators are also used and might ultimately be preferable for flexible electronics. The organic semiconductor film (∼30−50 nm thick) can be deposited from the vapor phase or coated from solution. If desired, surface treatments on the insulator may be used prior to deposition of the semiconductor layer. These treatments have been observed to have profound effects on the resulting thin film structure and electrical characteristics.[7,8] The metal source and drain electrodes are often vapor-deposited through a shadow mask, but conductive inks that can be printed are also employed. Source−drain channel lengths, $L$, shown in Figure 1c, typically range from 10 to 100 $\mu$m, and channel widths, $W$, are usually between 100 $\mu$m and 1 mm.

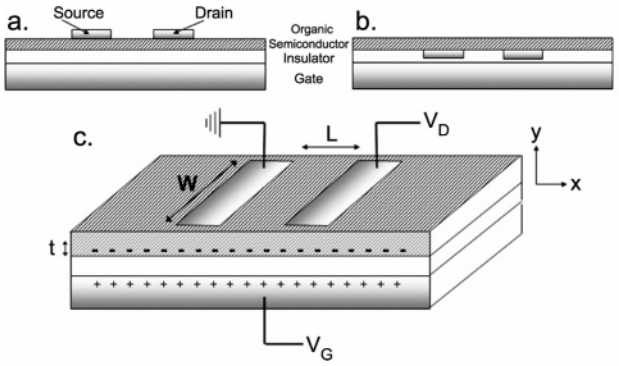


**Figure 1.** Schematic of top (a) and bottom (b) contact organic TFTs. (c) Relevant voltages and geometry for a TFT.

The voltage applied between the source and drain is referred to as the source−drain voltage, $V_D$. For a given $V_D$, the amount of current that flows through the semiconductor film from source to drain is a strong function of the voltage, $V_G$, applied to the gate electrode. The semiconductor film and the gate electrode are capacitively coupled such that application of a bias on the gate induces charge in the semiconductor film, as shown schematically in Figure 1c. Much of this charge is mobile and moves in response to the applied source−drain voltage $V_D$. Ideally, when no gate voltage is applied, the conductance of the semiconductor film is extremely low because there are no mobile charge carriers; i.e., the device is "off". When the gate voltage is applied, mobile charges are induced, and the transistor is on.

The origin of the gate-induced charging (also known as the "field effect") is clarified in the simplified electronic energy level diagrams shown in Figure 2. Figure 2a shows the positions of the highest occupied molecular orbitals (HOMOs) and lowest unoccupied molecular orbitals (LUMOs) of the organic semiconductor relative to the Fermi levels of the source and drain contacts. In this case, the gate bias is zero. If a small source−drain bias were applied, there would be no conduction because there are no mobile charges in the semiconductor. Parts b and d of Figure 2 show the situation when a positive gate voltage is applied with $V_D = 0$ and $V_D > 0$,

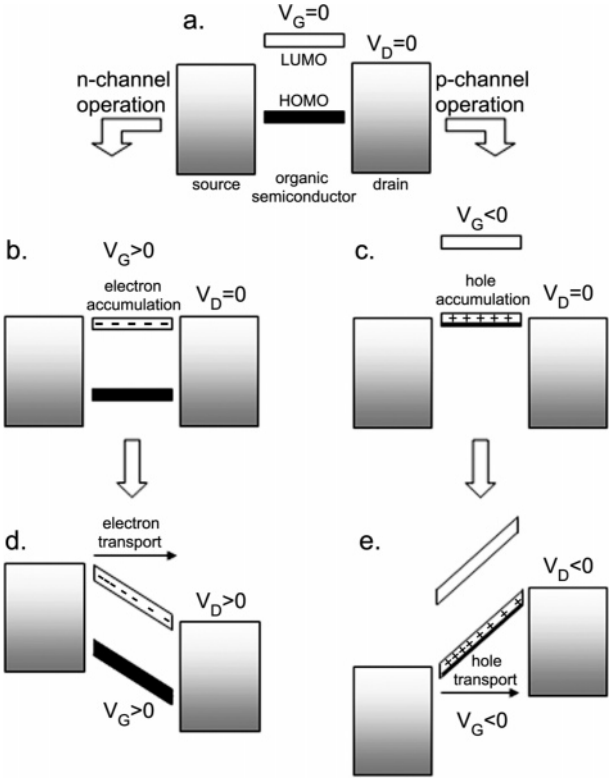


**Figure 2.** (a) Idealized energy level diagram of an organic TFT at $V_G = 0$ and $V_D = 0$. (b–e) demonstrate the principle of field effect transistor operation for the case of electron accumulation (b) and transport (d) and hole accumulation (c) and transport (e).

respectively. Application of a positive gate voltage produces a large electric field at the organic/insulator interface. This field causes the HOMO and LUMO levels in the semiconductor to shift down (lower in energy) with respect to the Fermi levels of the metal contacts, which remain fixed as their potentials are externally controlled. If the gate field is large enough, the LUMO will become resonant with the Fermi levels of the contacts, and electrons can then flow from the contacts into the LUMO, Figure 2b. Now there are mobile electrons at the semiconductor/insulator interface, which upon application of a drain voltage, Figure 2d, result in electric current between the source and drain. This same reasoning applies with negative gate bias, Figure 2c,e. Negative gate bias causes the HOMO and LUMO levels to shift up such that the HOMO becomes resonant with the contact Fermi levels and electrons spill out of the semiconductor and into the contacts, leaving positively charged holes. These holes are now the mobile charges that move in response to an applied drain voltage, Figure 2e. Note that in Figure 2d,e the source electrode is always the charge-injecting contact regardless of the sign of the gate voltage.

The diagrams in Figure 2 are a useful way to visualize the mechanism by which conduction in OTFTs is modulated by the gate electrode. However, this description is simplistic, and a quantitative description of the process must account for the presence of charge traps and residual dopants, for example. In addition, the diagrams in Figure 2 might lead one to believe that any organic semiconductor can be made to conduct holes or electrons, depending on the sign of the gate voltage. This

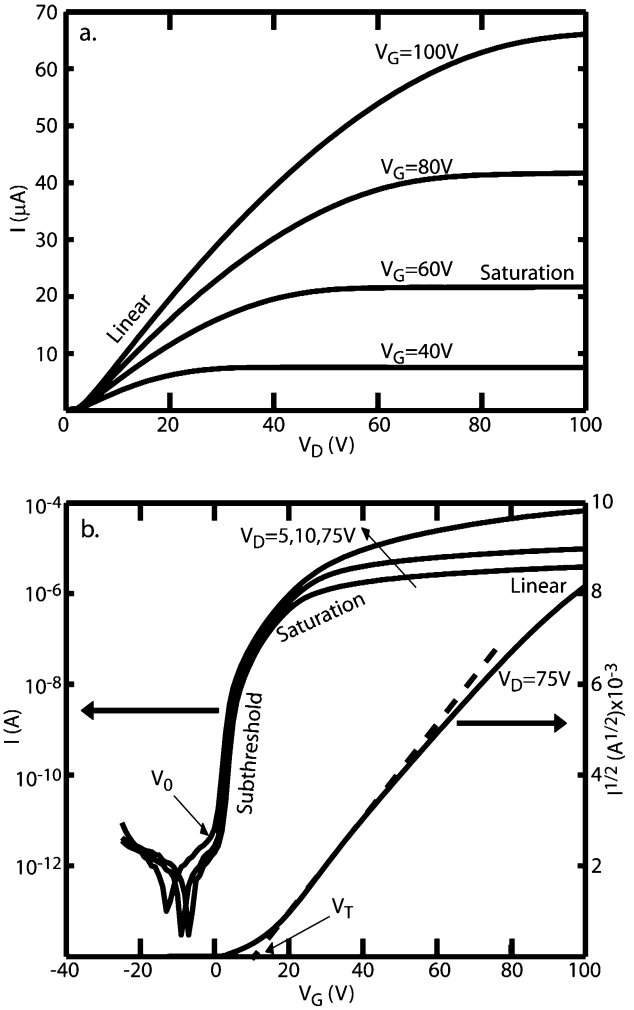


**Figure 3.** (a) Example $I_D-V_D$ curves for a PTCDI-$C_8$ TFT for various values of $V_G$. (b) Example $I_D-V_G$ curves plotted on semilogarithmic axes for the same device for various values of $V_D$. The $I^{1/2}$ vs $V_G$ curve for $V_D = 75$V is shown on the right-hand axis.

is not true; in general, a given organic semiconductor can be made more conductive with either a positive or a negative gate voltage, but not both, with only a few recent exceptions. Hence, organic semiconductors are classified according to whether they are hole (p-channel) conductors or electron (n-channel) conductors.

TFTs are typically characterized in one of two ways, either by holding $V_G$ constant and sweeping $V_D$ (commonly referred to as $I_D-V_D$ or output curves; see Figure 3a) or by holding $V_D$ constant and sweeping $V_G$ (commonly referred to as $I_D-V_G$ or transfer curves; see Figure 3b). If contact effects and trapping are not too problematic, these traces can be modeled quantitatively using $I-V$ relationships derived from Ohm's law.

Looking again at Figure 2b for the case of n-type conduction and $V_D = 0$, if we assume ohmic contacts and zero-threshold operation (these assumptions will be qualified shortly), application of a positive $V_G$ induces positive charges at the gate/insulator interface and an equal number of negative charges near the organic/insulator interface (supplied by the source and drain contacts). With no source–drain bias applied, this negative charge density will be uniform across the channel. For a positive $V_D$ (Figure 2d) the areal density

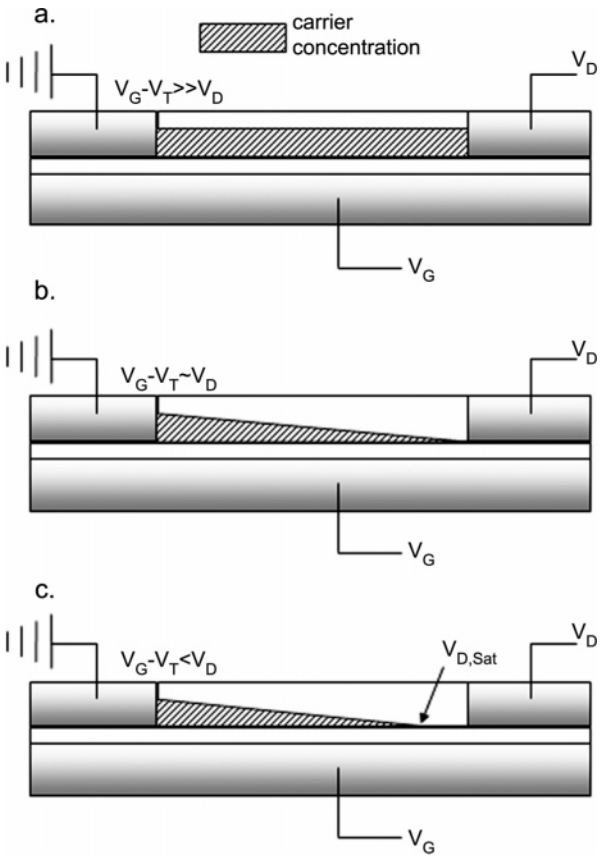


**Figure 4.** (a) Carrier concentration profile of TFT in the linear regime. (b) Pinch-off occurs when $V_D \approx V_G - V_T$. (c) Carrier concentration profile of TFT in the saturation regime.

of charge (C/cm$^2$) induced at a given position $x$ along the channel is proportional to the voltage difference $V_G - V(x)$:

$$q_{ind}(x) = n(x)et = C_{ox}(V_G - V(x)) \qquad (1)$$

where $C_{ox}$ is the capacitance of the insulator per unit area, typically reported in nF/cm$^2$, $n(x)$ is the number density of charges in the channel (no./cm$^3$), $e$ is the fundamental unit of charge, and $t$ is the thickness of the charged layer in the channel.

More often than not, the point at which mobile charge carriers are first introduced into the organic film does not correspond to $V_G = 0$. For an n-channel semiconductor, a mismatch between the Fermi level of the metal and the organic LUMO (analogous to the conduction band for conventional semiconductors) results in charge transfer between the metal and organic, causing a dipole and band bending in the organic. This necessitates the application of a nonzero $V_G$ (often referred to as $V_{FB}$ in the literature) just to achieve the flat-band condition. Furthermore, if there are large numbers of deep electron traps present in the film (deep enough to render the electrons trapped in them effectively immobile), these will have to be filled before the channel can conduct. Conversely, if the channel is inadvertently doped with negative carriers (e.g., by remnant impurities), it will be conductive at $V_G = 0$.

To handle these various situations, it is convenient to define a threshold gate voltage, $V_T$, necessary to induce mobile charges. $V_T$ is a parameter that lumps together all the effects described in the preceding paragraph. For an n-channel material, doping the channel shifts $V_T$ negatively (in other words, the device has to be biased negatively to shut it off), deep traps shift $V_T$ positively, and mismatch between the LUMO and metal Fermi level can shift it in either direction depending on the nature of the misalignment. Including the threshold voltage, eq 1 becomes

$$q_{ind}(x) = n(x)et = C_{ox}(V_G - V_T - V(x)) \qquad (2)$$

Figure 4a shows that, when $V_D = 0$, the channel charge density is uniform for a given $V_G$ (since ideally $V_T$ is not a function of $x$, and when $V_D = 0$, $V(x) = 0$). However, when $V_D$ is nonzero but less than $V_G$, there is a *linear gradient* in the charge concentration, Figure 4b. For a given small value of $V_D$, the *average* value of $q_{ind}$ is $C_{ox}(V_G - V_T - V_D/2)$, which is the induced areal charge density in the center of the channel. To the left of center, the charge density will be higher, and to the right, the charge density will be lower.

Now we arrive at the $I-V$ relationship for a TFT in a simplistic fashion; a more rigorous derivation can be found in standard texts.[9] To begin, we simply write down Ohm's law and use the definition of conductivity:

$$\frac{I_D}{tW} = \sigma\frac{V_D}{L} \;\Rightarrow\; I_D = \frac{W}{L}(n_{ind,av}et)\mu V_D \qquad (3)$$

where $\sigma$ is the conductivity, $\mu$ is the carrier mobility (i.e., velocity per unit electric field), and $n_{ind,av}$ is the average carrier concentration in the channel. Substituting eq 2 into eq 3, we obtain

$$I_D = \frac{W}{L}C_{ox}\mu\left[(V_G - V_T) - \frac{V_D}{2}\right]V_D \qquad (4)$$

which is commonly rewritten as

$$I_D = \frac{W}{L}C_{ox}\mu\left[(V_G - V_T)V_D - \frac{{V_D}^2}{2}\right] \qquad (5)$$

Equation 5 is the standard "linear regime" equation, and it describes transport for the case shown pictorially in Figure 4b, where $V_D < (V_G - V_T)$. Equation 4 is easier to understand in that the terms inside the brackets multiplied by $C_{ox}$ give the average areal charge density in the channel; the higher the average charge density, the higher the drain current will be. Equation 5 shows that in the so-called linear regime the current scales linearly with the gate voltage and quadratically with the drain voltage. For $(V_G - V_T) \gg V_D$ it is approximately correct to drop the $V_D/2$ term.

For the purposes of calculating the field effect mobility in the linear region, it is useful to define two derivatives:

$$g_m = \left.\frac{\partial I_D}{\partial V_G}\right|_{V_D} = \frac{W}{L}C_{ox}\mu_{lin}V_D$$

$$g_d = \left.\frac{\partial I_D}{\partial V_D}\right|_{V_G} \sim \frac{W}{L}C_{ox}\mu_{lin}(V_G - V_T) \qquad (6)$$

when $(V_G - V_T) \gg V_D$.

These derivatives are referred to as the transconductance ($g_m$) and conductance ($g_d$), respectively. The mobility can be calculated from either of these derivatives for a given $V_D$ or $V_G$, or a composite linear region mobility can be calculated from the variation of $g_m$ with $V_D$ or $g_d$ with $V_G$:

$$\frac{dg_m}{dV_D} = \frac{dg_d}{dV_G} = \frac{W}{L} C_{ox} \mu_{lin} \tag{7}$$

Following one of the high-$V_G$ traces in Figure 3a, for $V_G - V_T \gg V_D$, the channel has a nearly uniform carrier concentration from source to drain (Figure 4a), and the current is approximately linear with $V_D$ in this region. As $V_D$ is increased, the carrier concentration profile becomes increasingly nonuniform, decreasing from the source to the drain electrode and resulting in quadratic $I-V$ characteristics. When $V_D = V_G - V_T$ (Figure 4b), the channel becomes "pinched". In other words, there is no longer a potential difference between the gate and the part of the channel nearest the drain electrode, resulting in a region near the drain completely depleted of free carriers. Further increases in $V_D$ serve only to push this pinch point slightly backward toward the source electrode (this effect has been exaggerated in Figure 4c). As long as the device length $L$ is much longer than the width of this depletion region, further increases in $V_D$ yield no additional current, since the integrated resistance of the channel from the source to the pinch point remains the same, and carriers are swept across the narrow space charge region from the pinch point to the drain by the (comparatively) high electric field in the depletion region. Substituting $V_D = V_G - V_T$ into eq 5 yields the equation describing the $I-V$ characteristics of a field effect transistor in saturation:

$$I_{D,sat} = \frac{W}{2L} C_{ox} \mu_{sat} (V_G - V_T)^2 \tag{8}$$

Therefore, the device mobility can also be calculated in the saturation region from the slope of a line drawn through the linear part of an $I_{D,sat}^{1/2}$ vs $V_G$ plot. This is shown in Figure 3b along with the $I-V$ characteristics on semi-logarithmic axes. A few things should be noted regarding analysis of the saturation characteristics. First, the mobilities calculated in the linear and saturation regions do not always agree; often $\mu_{sat}$ is higher. Since the integrated resistance of the channel is higher in saturation than in the linear region, contact resistances are likely to be less noticeable in this region. Ohmic contacts were assumed in deriving eq 4, but nonnegligible voltage drops near the contacts due to Schottky barriers and (in the case of top-contact devices) access resistances through the ungated portion of the organic semiconductor are almost invariably present in these devices.[10] Second, the threshold voltage $V_T$ can be calculated from the intercept of a line drawn through the linear region of the $I_{D,sat}^{1/2}$ vs $V_G$ plot. This is shown in Figure 3b. Here, and in most devices, one notices that this intercept does not always coincide with the exponential increase in current (designated $V_0$) shown on the adjacent logarithmic axes. In addition to deep traps that immobilize carriers at least as long as the measurement duration, there is inevitably also a distribution of shallower traps with release rates on the order of the measurement time. As $V_G$ is increased, more of these traps are filled and unavailable to trap subsequent carriers. As a consequence, the mobility in the saturation region appears to be a continuously increasing function of $V_G$, and this results in an offset between $V_0$ and $V_T$ (and thus renders $V_T$ little more than a fit parameter for these devices). In general, the higher the mobility of the device, the smaller this offset is, since low mobilities and large offsets are both symptomatic of high shallow-trap concentrations.

In addition to $\mu$ and $V_T$ (or $V_0$), two other metrics are often cited in evaluating TFT performance. The first is the on/off current ratio, $I_{ON}/I_{OFF}$, which is self-explanatory and is typically reported as $10^x$. Achieving a high on/off ratio generally translates to maximizing the mobility, which more or less determines $I_{ON}$, and minimizing the off current (due to dopants). The second is the subthreshold swing, $S$:

$$S = \frac{dV_G}{d(\log I_D)} \tag{9}$$

$S$ is a measure of how rapidly the device switches from the off state to the on state in the region of exponential current increase and is typically reported in V decade$^{-1}$ or mV decade$^{-1}$. A more useful metric for comparison between films deposited on different dielectrics or on dielectrics of varying thickness is the normalized subthreshold swing, $S_n = C_{ox}S$ (V nF cm$^{-2}$ decade$^{-1}$), which yields the required number of gate-induced carriers to effect a one-decade increase in the current near $V_0$ and thus allows meaningful comparison of films on different dielectrics. A large subthreshold swing generally implies a large concentration of shallow traps, i.e., a diffuse turn-on region. Both $I_{ON}/I_{OFF}$ and $S_n$ are dependent on the device geometry, operating conditions, and measurement apparatus (current detection levels in particular), and thus are only truly useful when cited along with this information or when used to compare devices tested under identical circumstances.

## 3. Literature Summary of n-Channel Organic Materials for Transistors

There are several reasons why development of high-performance n-channel organic TFT materials has lagged behind that of p-channel materials. The first is that the metals typically used for making contact to these materials (Au, Ag, and other noble metals primarily) have work functions better suited for injection of holes into the HOMO than of electrons into the LUMO for typical organic semiconductors. Low-work-function metals such as Al, Mg, or Ca, while expected to have lower electron injection barriers, oxidize easily and readily form reactive complexes with the organic semiconductor.[11] Second, unsubstituted oligothiophenes and oligoacenes have relatively small electron affinities (~2.8 eV for pentacene in the solid state[12]). Usually, these molecules have to be augmented with electron-withdrawing side groups to stabilize the anionic forms of the molecule and allow them to efficiently transport negative charges. Even if the molecule can be chemically tailored to exhibit n-channel conduction, the susceptibility of organic anions to atmospheric oxidants such as $O_2$ and $H_2O$ remains a problem.[13] Electronically, this

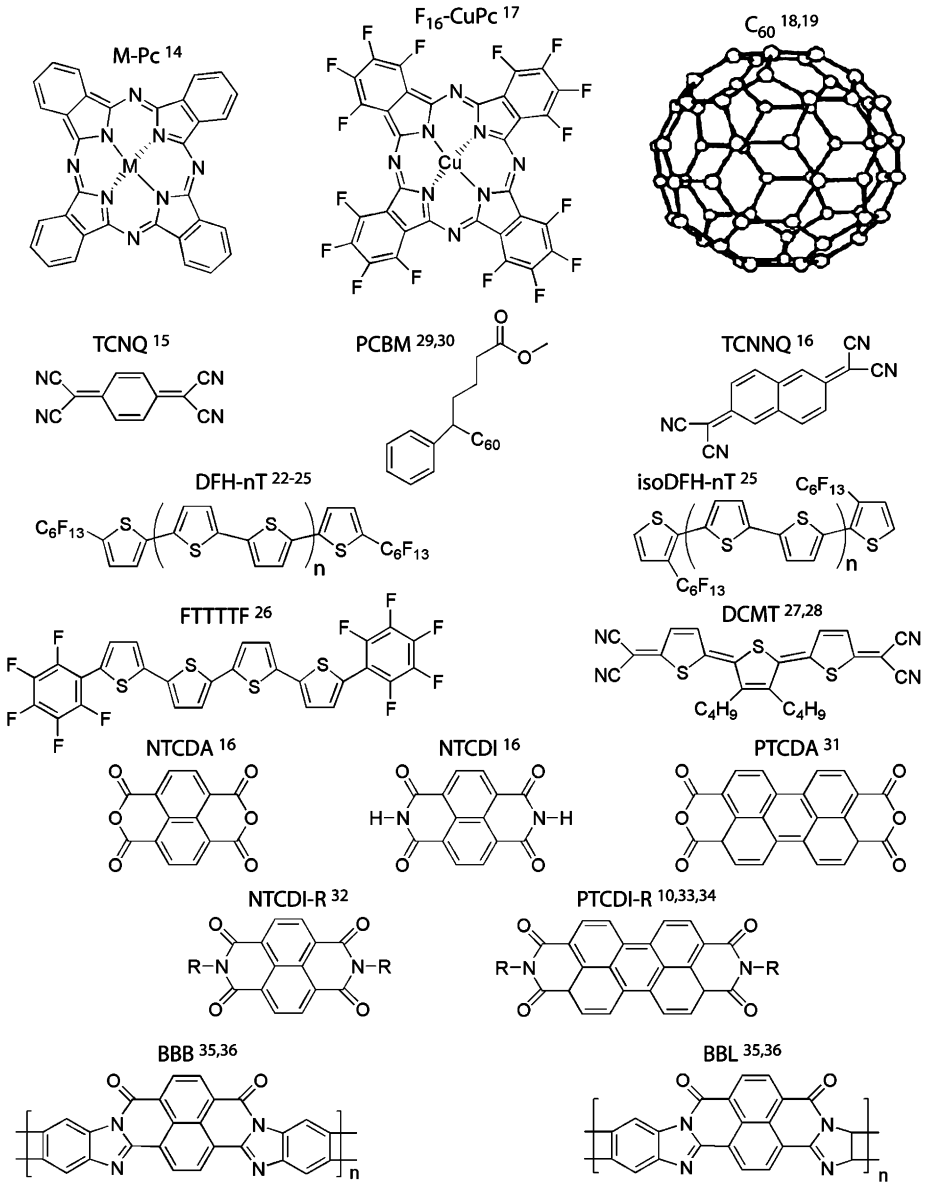


**Figure 5.** Structures of n-channel semiconductors with known TFT characteristics.

susceptibility may manifest itself in the formation of efficient electron traps or the sharp degradation of transport properties upon exposure to air. Therefore, the area of n-channel organic semiconductors involves not only maximizing the mobility of these materials but also minimizing the deterioration of electronic properties over time.

Dimitrakopoulos and Malenfant have summarized the progress in the area of molecular n-channel organic semiconductors for thin film applications from the first work using metal-phthalocyanines in 1990 to the achievement of electron mobilities of $\sim$0.6 cm$^2$ V$^{-1}$ s$^{-1}$ in 2001.[3] The purpose of this section is to summarize the progress that has been made since then in small-molecule n-channel organic semiconductors, to summarize the work in n-channel polymeric semiconductors (an area in which considerably less work has been done), and to discuss potentially useful n-channel materials which have not yet been fully tested as the active layer in TFTs.

Figure 5 shows the molecular structures of n-channel organic semiconductors that have been characterized in a TFT configuration, both molecular and polymeric, most of which are constructed via the addition of electron-withdrawing groups (cyano, perfluoroalkyl, etc.) to known p-type cores (naphthalene, perylene, 6T, etc.). Many have been discussed in ref 3 and will only be briefly revisited here. Early work with the rare-earth-metal/organic complexes $Pc_2Lu$ and $Pc_2Tm$ yielded devices with mobilities of $\sim 10^{-4}$ cm$^2$ V$^{-1}$ s$^{-1}$, and in the case of $Pc_2Lu$, ambipolar (electron and hole) transport was observed after annealing.[14] TCNQ and TCNNQ, both of which have received considerable attention as the acceptor half of organic/metal complexes, yielded electron mobilities of $\sim 10^{-5}$ and $10^{-3}$ cm$^2$ V$^{-1}$ s$^{-1}$, respectively, in single-component thin films.[15,16] All of these mobilities were measured under vacuum, and in all cases the electrical properties were reported to degrade quickly when the complexes were exposed to air. In the case of $Pc_2Lu$, n-channel conduction was completely suppressed upon breaking of the vacuum. In 1998, Bao et al. demonstrated that the addition of strong electron-withdrawing groups to metallophthalocyanines could result in air-stable n-channel organic

semiconductors. A mobility of 0.03 $cm^2\ V^{-1}\ s^{-1}$ in air was reported for the perfluorinated $F_{16}CuPc$.[17]

As of 2000, the highest reported electron field effect mobility in an organic thin film was for $C_{60}$ on an amine-modified surface[18] ($\mu \approx 0.3\ cm^2\ V^{-1}\ s^{-1}$), but the performance of these films degraded rapidly upon exposure to air. Recently, Kobayashi et al. reported mobilities as high as 0.56 $cm^2\ V^{-1}\ s^{-1}$ for $C_{60}$ films fabricated by molecular beam deposition, but these mobilities could only be achieved by performing device fabrication and electrical characterization without breaking the vacuum.[19]

Oligothiophenes constitute one of the most extensively characterized series of p-channel molecules,[20,21] but a number of groups have demonstrated that the oligothiophene backbone can be used as a foundation for building n-channel organic semiconductors. Facchetti et al. have synthesized a series of n-channel semiconductors by adding perfluorohexyl groups ($C_6F_{13}$) to the $\alpha,\omega$ (DFH-*n*T) or $\beta,\beta'$ (isoDFH-*n*T) positions of oligothiophenes, where $n = 0$, 0.5, 1, 1.5, or 2. The highest observed mobility in these materials is $\sim$0.05 $cm^2\ V^{-1}\ s^{-1}$ for thermally evaporated DFH-4T films.[22−25] This same group has also synthesized n-channel semiconductors based on permutations of thiophene and fluoroarene groups. Electron mobilities as high as 0.08 $cm^2\ V^{-1}\ s^{-1}$ have been observed in FTTTTF.[26] All of these mobilities were measured in vacuum.

Chesterfield et al. have recently reported on the electrical characterization of the n-channel organic semiconductor DCMT, a quinoid terthiophene derivative with electron-withdrawing dicyanomethylene groups. Mobilities as high as 0.2 $cm^2\ V^{-1}\ s^{-1}$ were observed under vacuum in the best films of DCMT.[27,28] These high-mobility films showed only n-channel behavior, but other films of this same material exhibited both p- and n-channel behavior,[28] although the mobility for both carrier types in these films was significantly lower. Ambipolar device operation has also been achieved in two-component solution-cast organic TFTs. The n-channel material in these films (with $\mu \approx 0.02$) was the $C_{60}$ derivative PCBM.[29] This same material has also been solution-cast in single-component n-channel TFTs with mobilities as high as $5 \times 10^{-3}\ cm^2\ V^{-1}\ s^{-1}$.[30]

The most extensive work thus far on n-channel molecular organic semiconductors has involved compounds formed by adding electron-withdrawing dianhydride or diimide moieties to naphthalene and perylene cores (NTCDI-R and PTCDI-R in Figure 5). The earliest attempts to fabricate TFTs from these materials yielded mobilities of $\sim 10^{-3}$ and $10^{-4}\ cm^2\ V^{-1}\ s^{-1}$ for NTCDA and NTCDI,[16] respectively, and $\sim 10^{-4}\ cm^2\ V^{-1}\ s^{-1}$ for thin films of PTCDA.[31] Later, Katz et al. demonstrated that the mobility and air stability of these devices could be greatly improved by incorporating various *N*,*N*′ substituents on NTCDI. In particular, it was found that fluorinated side groups ($R = CH_2C_6H_4CF_3$ in this case), which may act as a kinetic barrier to the diffusion of oxidizing species, yield devices with mobilities $>0.1\ cm^2\ V^{-1}\ s^{-1}$ in air.[32] In 2001, Malenfant et al. demonstrated mobilities of 0.6 in PTCDI-$C_8$ in a vacuum, but the threshold voltage in this device was $\sim$75 V, indicating a large concentration of traps.[33] Recently, Chesterfield et al. have demonstrated saturation mobilities as high as 1.7 $cm^2\ V^{-1}\ s^{-1}$ in the same molecule, and with threshold voltages of 10−15 V.[34] Chesterfield et al. investigated the effect of the alkyl chain length ($C_5$, $C_8$, and $C_{12}$)[34] on device characteristics and the effect of various metals on contact resistance and device performance of thin films of the $C_5$ derivative.[10]

The literature on n-channel semiconducting polymers for TFT applications is significantly sparser than for oligomeric materials. Most of the work on semiconducting polymer TFTs has focused on p-channel materials such as regioregular poly(3-hexylthiophene) (P3HT), for which mobilities as high as 0.1 $cm^2\ V^{-1}\ s^{-1}$ have been observed. To the best of our knowledge, the work of Babel and Jenehke on the polymers BBL and BBB represents the only available information on intrinsic n-channel conduction in polymer TFTs.[35,36] An electron mobility of $\sim 0.1\ cm^2\ V^{-1}\ s^{-1}$ was observed in a solution-cast film of BBL in air, but only $10^{-6}\ cm^2\ V^{-1}\ s^{-1}$ was observed for similarly fabricated BBB films.

In addition to compounds with known transistor properties, there are a number of relatively new molecular and polymeric materials whose potential as n-channel semiconductors has been gauged by their structural similarity to known n-channel organics,[37] their electrochemical and spectroscopic properties,[38−46] and their electrical performance in alternative device structures such as Schottky diodes or organic light-emitting diodes (OLEDs).[39,40,42,43,47] Figure 6 shows a handful of these structures. DB-TCV3T, the aromatic analogue of the quinoid DCMT, exhibits a field effect mobility of $\sim 0.02\ cm^2\ V^{-1}\ s^{-1}$, while PTCDI-PPEEB, which shows liquid crystalline behavior, exhibits mobilities of $\sim 0.05\ cm^2\ V^{-1}\ s^{-1}$ in preliminary thin film work.[48] Electron mobilities as high as 0.6 $cm^2\ V^{-1}\ s^{-1}$ have been observed in DFHCO-4T recently, and ambipolar transport (with n- and p-channel mobilities of $\sim 10^{-3}$) has been observed in thin films of DHCO-4T.[49]

## 4. Materials Requirements for n-Channel Organic Semiconductors

In this section, we discuss the properties that organic semiconductors must have to function as good n-channel materials in OTFTs. At the outset of this discussion, it is worth making the point that the transport mechanism in OTFTs is not clear. There are essentially two limiting case models, (1) carrier hopping and (2) multiple trapping and release (MTR),[50] and the list of materials requirements for n-channel conduction depends somewhat on which mechanism is operating. Nevertheless, there are important characteristics that are clearly necessary no matter which transport model is correct. On the basis of this and the experiences of researchers in this area, it is possible to assemble lists of both necessary and desirable properties.

**4.1. Necessary Properties.** *4.1.1. Conjugated π-Electron System with High Electron Affinity (>3.0 eV).* All organic semiconductors are made from molecules that are highly conjugated and rich in $\pi$-electrons; there are several reasons for this. The first reason is that the $\pi$-orbitals are energetically accessible for electrical transport. For example, for typical p-channel materials, the ionization potentials associated with electrons in the HOMO are about 5 eV, far smaller than the 10 eV ionization energies common to alkanes. Practically

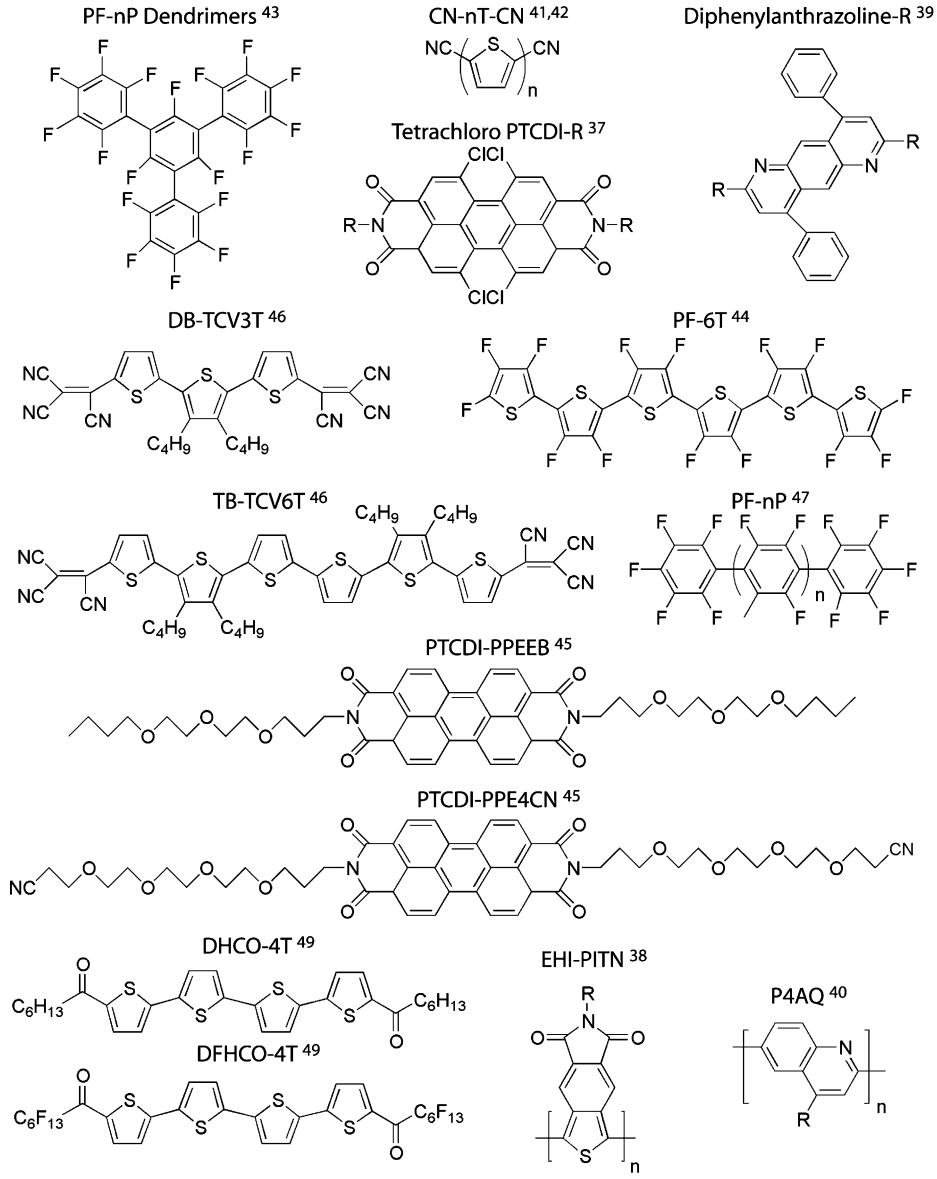


**Figure 6.** Structures of n-channel semiconductors with unknown or unpublished TFT characteristics.

speaking, this means it is possible to inject positive charge (holes) from metal electrodes (particularly high-work-function metals) into films of conjugated p-channel molecules. A second reason is that, once a charge is placed on a conjugated molecule, it is rapidly delocalized over the $\pi$-orbital system. This of course leads to extremely fast conduction within the molecule, but more importantly, the delocalization also facilitates transport of charge between molecules (intermolecular charge transfer) by maximizing the spatial overlap of the delocalized charge with the electronic states on an adjacent molecule.

For n-channel materials, it is the *electron affinity*, not the ionization potential, which must be high enough to allow efficient injection of electrons into the empty LUMO of the semiconductor molecules. It appears that from a practical standpoint the electron affinity needs to be at least 3.0 eV, but should not be much greater than 4.0 eV. The reason for the upper limit, which is difficult to achieve anyway, is that if the molecule is too electrophilic its stability in ambient conditions will be overly compromised. For example, films of electrophilic molecules can "air-dope" by reaction with atmospheric moisture, and such doping is not desirable for OTFT performance.

*4.1.2. Good Intermolecular Electronic Overlap*. For intermolecular charge transport to be fast, overlap between wave functions on adjacent molecules must be as large as possible. This is naturally a function of the type of bonding between the semiconductor molecules, but it also depends on the size of the molecules, the molecular symmetry, and the symmetry of the crystal packing.[51] The critical role of electronic overlap and its dependence on the packing geometry is discussed in detail in section 5, so we will not discuss it further here. However, it is important to note that in many crystalline organic semiconductor materials there are *two* major contributions to intermolecular bonding, the dispersion and the quadrupolar interactions. The role of dispersive interactions is generally well recognized, and consequently, some workers refer to crystalline organic semiconductors as "van der Waals" solids, though this is often an inaccurate characterization. In contrast, the importance of the quadrupolar interaction is frequently neglected in the organic electronics literature. The quadrupolar interaction arises from the charge polar-

ization present within many rigid aromatic systems. Benzene ($C_6H_6$), for example, has a quadrupole moment (think of two back-to-back dipoles) stemming from the combination of the net negative charge in the $\pi$-clouds above and below the plane of the molecule and the net positive charge from the exposed protons on the periphery of the benzene ring. In the solid state, benzene packs "edge-to-face" such that a proton on one ring interacts strongly with the $\pi$-system on an adjacent ring. In this case, the quadrupolar interaction completely dominates the interaction energy. On the other hand, the crystal structure of pentacene, an archetypal p-channel organic semiconductor, results from the interplay of strong dispersive interactions between the delocalized $\pi$-orbitals, which favor face-to-face $\pi$-stacking, and the quadrupolar interaction, which favors edge-to-face packing. Determining how these two different types of intermolecular interactions affect intermolecular orbital overlap is an important area of research.[52,53]

*4.1.3. Good Film-Forming Properties*. Efficient transport of charge through a semiconductor film requires that the film be continuous and ordered. In the case of vapor-deposited, low-molecular-weight organic semiconductors that form polycrystalline films, it is necessary that there be good connectivity between the grains. It is also important that the polycrystalline film be highly oriented so that the fast transport directions in the grains lie parallel to the dielectric surface; highly oriented polycrystalline films display higher carrier mobilities than amorphous films or randomly oriented crystalline films.[3] In the case of solution-processed films (small molecules or polymers), comparable crystallinity is not achieved, meaning there are amorphous domains with presumably lower carrier mobilities.[54] Chain orientation is certainly possible in the case of polymers and is desirable for transport. The quality of solution-cast films depends strongly on the solubility of semiconducting molecules in a given solvent, and this continues to pose challenges for solution processing, as discussed further below.

*4.1.4. Chemical Purity*. Chemical impurities in organic semiconductors for OTFT applications are undesirable for two reasons. First, impurities can result in charge-trapping sites in organic semiconductor films, which lowers the average mobility and degrades the OTFT on current and threshold (onset) voltage stability. Second, impurities can function as dopants, thereby increasing the conductivity of the film in the off or ungated state, which results in large leak currents, excessive power dissipation, and low on-to-off current ratios. Thus, it is important to work with organic semiconductors that are as pure as possible, and this remains a major challenge for organic electronics because of the complexity of the synthetic processes used to make the materials and the large number of different types of impurities that can be present.

*4.1.5. Stability*. Stability refers to the time variation of OTFT performance parameters such as $V_T$, $\mu$, $I_{ON}/I_{OFF}$, and $S$, and it is profoundly affected by the purity, chemical sensitivity, and microstructure of the organic semiconductor film. Stability is also a function of the details of device operation, e.g., how long the device is turned on at any given time. A common problem encountered with OTFTs is threshold voltage shift (TVS),[55,56] wherein prolonged device operation results in trapped charge at the dielectric/film interface, which subsequently modifies the gate threshold voltage to turn the device off and on. A consequence of TVS is hysteresis in $I_D-V_D$ and $I_D-V_G$ curves.

A principal issue, particularly for n-channel conductors, is air stability. Many n-channel OTFTs show significant degradation in performance when operated in air. This necessitates device encapsulation, which introduces an undesirable extra processing step, and means that the OTFT will have a limited lifetime because the encapsulation is never perfect. De Leeuw and colleagues have considered the issue of air stability in terms of the formal redox potentials for $H_2O$, $O_2$, and specific organic semiconductors.[13] The chief problem is that the anions of organic semiconductor molecules, which are formed at positive gate voltages, have large reducing power and can reduce or complex with $O_2$ and $H_2O$ molecules that have diffused into the film. This means that the charged states of n-channel organic semiconductors are thermodynamically unstable in the ambient and methods must be found to prevent the diffusion of air into the active channel region (kinetic control), to limit the solubility of $O_2$ and $H_2O$ in the film (thermodynamic control), or to block the chemical reaction between $O_2$ and the semiconductor molecules (chemical/kinetic control). The preparation of air-stable n-channel organic semiconductors remains a major challenge, but there has been some recent success with semiconductor molecules having fluorinated functionalities, $F_{16}CuPc$[17] and NTCDI-R[32] (with R = $CH_2C_6H_4$-$CF_3$), that apparently provide a kinetic barrier to the diffusion of atmospheric contaminants in the film. Of the molecules shown in Figures 5 and 6, only these two have demonstrated air-stable operation.

**4.2. Desirable Properties.** *4.2.1. Solution Processability*. Thermal evaporation of organic semiconductors under vacuum typically yields thin films of the highest possible quality in terms of purity, grain size, and crystallinity. Although these films are useful for investigation of intrinsic transport properties and in establishing upper performance thresholds, to fully realize the cost advantages associated with organic semiconductors, one would prefer to work with solution-based deposition processes such as spin-coating and inkjet printing.[57] Unfortunately, many organic semiconductor molecules such as pentacene and sexithiophene have very poor solubility and are thus not amenable to these deposition methods. Techniques for circumventing this problem, such as depositing soluble precursors or adding solubilizing functionalities, have been used with some success.[58,59] The electron-withdrawing substituents added to p-channel cores to make them n-channel typically improve the solubility of the molecule. Further attempts to chemically improve the solubility, such as the addition of alkane side chains to molecules, need to be weighed against the effect these changes will have on crystal packing and film formation properties. As will be discussed later for DCMT (Figure 5), the effects of these solubilizing side groups on film structure can be significant.

*4.2.2. Low Carrier Trap Density*. From temperature-dependent mobility measurements in n-channel OTFTs, it has been found that the transport mechanism in these

devices can be well described as thermally activated trap-limited transport and not as coherent bandlike transport in extended states.[10,28] However, the nature and physical distribution of these traps are less clear. They may be highly localized at the semiconductor/insulator interface or at grain boundaries. Alternatively, the dominant trap states may be distributed, more or less homogeneously, within the grains themselves in the form of chemical or physical defects. Minimization of chemical defects was discussed earlier in the context of improving the purity and stability of the molecular film. For traps concentrated at interfaces or grain boundaries or transport limited by physical defects within the grain, mobility improvements will most likely be achieved through improvements in thin film crystallinity, i.e., searching for semiconductor/insulator systems and deposition conditions which yield large, highly perfect grains and few "in gap" interface states. The quality of the film within the first 5 nm from the dielectric is most critical as this is where the majority of charge resides in an OTFT.

Alternatively, the limiting trapping process in these films may be self-trapping (intrinsic hopping mechanism even in the absence of extrinsic traps/defects). This may occur in systems in which the average carrier residence time on a lattice site is comparable to the associated relaxation times, which is again a signature of trap-limited transport.[12,60] In such cases, deformation of the lattice around the charged site (i.e., polaron formation) and of the charge-bearing molecule itself may be responsible for the observed thermally activated behavior. Here, minimizing the molecular reorganization energy, $\lambda$, is an important consideration. This parameter will be explained in detail in section 5.

*4.2.3. Ohmic Contacts*. In the earlier derivation of the TFT equations, it was implicitly assumed that the organic semiconductor channel was the only significant resistance present in the device. However, many studies on both p- and n-channel OTFTs have shown significant nonohmic behavior at the metal/organic contacts.[61−63] Explanations for this include energy level offset between the metal and organic (i.e./ between the LUMO and the metal Fermi level for n-channel materials and between the HOMO and metal Fermi level for p-channel materials), alternative growth modes of the organic on the metal and insulator in the case of bottom-contact structures,[8] and geometry-related access resistances in the case of top-contact structures.[10] Curiously, for n-channel devices, low-work-function metal contacts such as Al and Mg (which should be superior electron injectors) are often outperformed by higher work function noble metals such as Au. This may be due to effects involving metal reactivity and interdiffusion at the metal/organic interface, leading to gap states that complicate the interfacial electronic structure.[11] For inorganic semiconductors such as Si, ohmic contacts are achieved by locally doping Si using standard lithographic techniques. This strategy has also been employed to make low-resistance contacts to organic semiconductors in OTFTs.[64,65]

## 5. Electronic Structure Considerations

Here we discuss more thoroughly the aspects of molecular and intermolecular electronic structure that affect the efficiency of transport in organic semiconductors. In $\pi$-conjugated systems, a strong pairing exists between the geometric and electronic structures; this pairing ultimately controls the transport properties.[66,67] Charge injection or electronic excitation processes indeed lead to (subpicosecond) geometry relaxations, which in turn modify the electronic structure.[60] In a transport regime corresponding to hopping, such as that often operational around room temperature in (disordered) $\pi$-conjugated materials, this coupling leads to a localization of the charge carriers on individual molecules for a time long enough that the nuclei can relax to the optimal geometry of the charged state.[68]

Importantly, at the microscopic level, the charge-transport mechanism can then be described as involving a self-exchange electron transfer from a charged oligomer to an adjacent neutral oligomer. In the context of semiclassical Marcus electron-transfer theory (as well as fully quantum mechanical extensions thereof),[69,70] the electron-transfer rates for self-exchange reactions may be written as

$$k_{et} = \left(\frac{4\pi^2}{h}\right) t^2 \frac{1}{(4\pi\lambda_B T)^{1/2}} \exp\left(\frac{-\lambda}{4k_B T}\right) \qquad (10)$$

These rates (and therefore the charge carrier mobilities) are determined by two major parameters.[51,71,72]

(i) The first one is the electronic coupling (transfer integral $t$) between adjacent molecules, which needs to be maximized; for instance, the electronic couplings have recently been shown to be large for pentacene, leading to electron and hole bandwidths on the order of 0.5 eV.[51,73]

(ii) The second one is the reorganization energy $\lambda$, which needs to be small for efficient transport, and which contains an inner part and an outer part. The inner reorganization energy for self-exchange reactions essentially corresponds to the sum of geometry relaxation energies in the molecule upon going from the neutral-state geometry to the charged-state geometry and vice versa; these two relaxation energies are usually nearly identical.[74] The outer reorganization energy deals with the medium polarization and is typically on the order of tenth(s) of an electronvolt.

We note that our experience with regard to reorganization energy is that molecules/oligomers that allow for fully delocalized HOMO and/or LUMO orbitals generally present low inner reorganization energies, on the order of 0.1 eV or less; this is for instance the case of pentacene, as well as several discotic liquid crystalline conjugated cores. It is also worth stressing that, in very well ordered materials, the charge carriers can be delocalized over many sites, with residence times on any given site that are shorter than the typical geometry relaxation times; in such instances, the reorganization energies vanish and a band regime can be attained in the absence of chemical or structural defects. In the remainder of this section, we will turn most of our attention to the electronic coupling aspects.

**5.1. Model Systems.** It has been shown that the transfer integral $t$, which describes the strength of the interactions (electronic coupling) between adjacent molecules/oligomers, can be estimated to a very good approximation for hole (electron) transport as half the

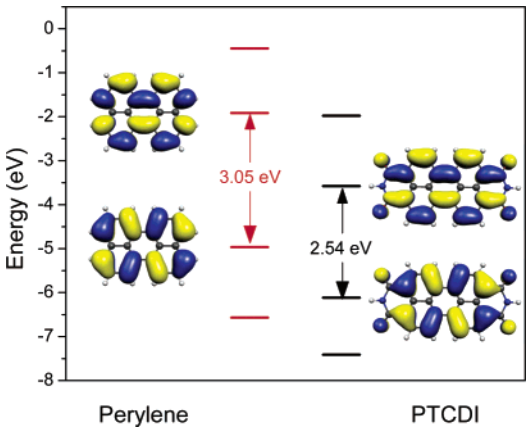


**Figure 7.** Upper two occupied and lower two unoccupied molecular orbitals of perylene and PTCDI calculated at the B3LYP/6-31G(d,p) level.

splitting of the HOMO (LUMO) level when a dimer made of two neutral molecules is considered.[51,75−77] When one-dimensional stacks of such molecules/oligomers are built, the widths of the corresponding valence and conduction bands can also be expressed as a function of the transfer integral and are equal to 4 times the respective $t$ integral.[51,75] Thus, knowledge of the transfer integrals is important in the context of both the band regime and the phonon-assisted hopping regime for charge transport.

Good insight into intermolecular/interchain transfer integrals can be obtained by considering the simple case of a dimer made of two chains (such as oligothiophene or polyene chains), either exactly superimposed on top of one another or laterally displaced with respect to one another, by translating one of the chains along its long or short axis (see ref 51). These calculations lead to the following conclusions.

(i) Perfectly cofacial configurations provide the largest electronic interactions (coupling) between adjacent molecules/oligomers. In perfectly cofacial stacks, the valence bandwidth is expected to be larger for small oligomers and the conduction bandwidth larger for long oligomers, with the valence bandwidth always larger than the conduction bandwidth. As described earlier, such configurations are made unstable by electrostatic interactions that lead to parallel displaced or herringbone configurations.

(ii) Importantly, small deviations from cofacial configurations often occur, and these drastically alter the values of the splittings and lead to situations where the electronic splitting becomes larger for the LUMO than for the HOMO.

**5.2. Perylene Derivatives.** As a first step, to understand the impact of the derivatization by electron-withdrawing groups on the electronic structure of the perylene core, we compared the highest two occupied orbitals and the lowest two unoccupied orbitals for perylene and perylene diimide, PTCDI (calculated on the basis of geometries optimized at the DFT/B3LYP level[78] with a 6-31G(d,p) basis set). By optimizing the cation and anion states, we also evaluated the effect of the withdrawing groups on the vertical and adiabatic ionization potentials (IPs) and electron affinities (EAs).

Figure 7 shows, as expected, that the effect of the withdrawing groups is to stabilize both the occupied and the unoccupied energy levels.[79,80] The vertical IP (EA) evolves by 1.00 eV (1.81 eV) from 6.43 eV (−0.46 eV) to 7.43 eV (−2.27 eV) upon addition of the electron-withdrawing groups to the perylene molecule (we note that IP and EA were calculated according to their definition, that is, from the difference in total energy between the ionized state and the ground state, and not using Koopmans' theorem, which considers the HOMO or LUMO level energies). Since the withdrawing groups more strongly influence the LUMO level, the stabilizations of the HOMO and LUMO are not equivalent (stronger for the LUMO), which leads to a reduction in the HOMO−LUMO gap. We note that the lowering of the LUMO level is expected to favor electron injection and to make the charged material more stable with respect to oxygen (in many instances, electron mobility can be hampered by the presence of oxygen which traps the negative charge carrier). Recently, Facchetti et al.[26] reported n-channel transport in oligo(thiophene−perfluorophenylene) and pointed out that the perfluoro substitution on electron-rich thiophene rings should lower LUMO energies, thus allowing more favorable electron injection.

We also evaluated the electronic structure of PTCDI-$C_5$, obtained by replacing the hydrogen atoms attached to the nitrogen atoms by pentyl chains. As one would expect, no significant variation in electronic properties is obtained compared to those of PTCDI. However, although the electronic structure of the individual molecules hardly changes when the nature of the moieties attached to the nitrogen atoms is modified, the derivatizations can result in major variations in solid-state packing and electronic properties. These modifications have been discussed earlier by Klebe et al.[81] and by Kazmaier et al.[82] and are referred to as the crystallochromic effect: differently substituted perylenes show closely related absorption spectra in a molecular dispersion (for instance, in polystyrene); however, the absorption maxima of the same series of compounds in the solid state spread over a range of more than 170 nm. The possibility of altering the packing (and thus of changing the electronic coupling between molecules) without changing the electronic properties of the individual molecules implies that the chemical flexibility of the perylene diimides can be used to tune the transport properties of these systems.

To exemplify how the crystal packing can change the electronic coupling between the molecular units, we computed the HOMO and LUMO transfer integrals, $t_{HOMO}$ and $t_{LUMO}$, for PTCDI and its PTCDI-$C_5$ derivative. The solid-state packing in both cases leads to displaced cofacial configurations with displacements along both the long and short molecular axes. The electronic couplings (HOMO and LUMO splittings) have been computed using clusters of molecules generated using the crystallographic data available in the Cambridge Structural Database for PTCDI and PTCDI-$C_5$[83] with the help of the semiempirical INDO Hamiltonian, developed by Zerner and co-workers.[84,85] The dominant electronic couplings are found along the $\pi$-stack direction (although nonnegligible interactions are also obtained for molecules on different $\pi$-stacks, indicating that two-dimensional transport is possible).

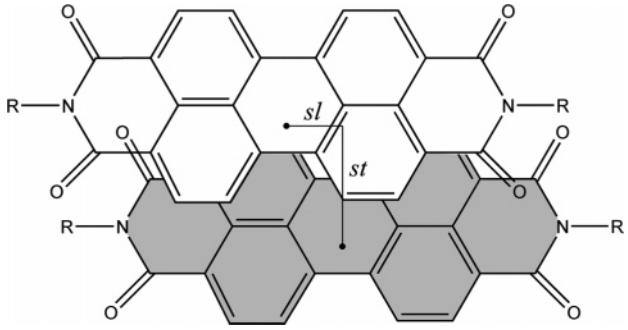


**Figure 8.** Transverse offsets in PTCDI-R defining two orthogonal slip directions.

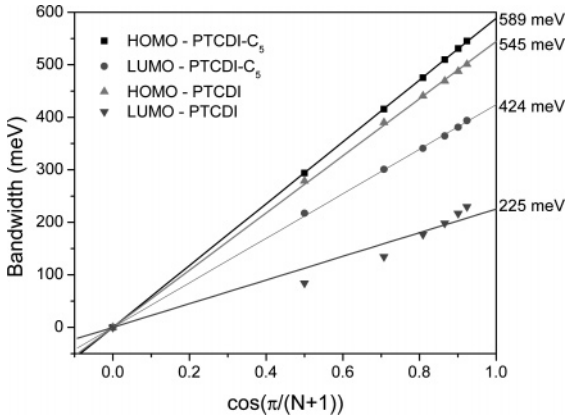


**Figure 9.** Evolution of the intermediate neglect of differential overlap (INDO) calculated bandwidths formed by the HOMO and LUMO levels of PTCDI and PTCDI-$C_5$ along the $\pi$-stacking direction as a function of $\cos(\pi/(N+1))$, with $N$ being the number of interacting molecules. The extrapolated bandwidths for an infinite stack were obtained by fitting the data points and are also indicated in the plot (far right).

The stacking distance, $d$, between adjacent molecules and the long-axis, sl, and short-axis, st, displacements are equal to[81] 3.343, 3.11, and 1.31 Å in PTCDI-$C_5$ and to 3.342, 3.37, and 1.10 Å in PTCDI, respectively. The larger offset difference is 0.21 Å. These differences are the main source of the large change in the LUMO bandwidth, shown in Figure 8.

Figure 9 illustrates that, on going from PTCDI to PTCDI-$C_5$, the difference in packing leads to an increase in HOMO bandwidth by less than 10% while the LUMO bandwidth nearly doubles. As pointed out in the detailed study published by Kazmaier and Hoffmann,[82] this is a consequence of the differences in the nodal characters of the HOMO and LUMO.

Larger modifications in the long- and short-axis offsets were reported by Klebe et al.[81] in a study involving 16 different perylene derivatives. A comparison between the theoretical and experimental data for these systems is under way; it promises to provide more insight into the structure−property relationships and to enable a better design of molecules for specific transport properties.

## 6. A Case Study: Development of n-Channel OTFTs Based on a $\pi$-Stacking Quinoidal Terthiophene Derivative

Three recent papers have reported the synthesis and properties of a new quinoidal oligothiophene, 3′,4′-dibutyl-5,5″-bis(dicyanomethylene)-5,5″-dihydro-2,2′:5′,2″-terthiophene (DCMT), Figure 5.[27,28,86−88] DCMT was designed to $\pi$-stack and incorporate *intra*molecular charge transfer to facilitate n-channel and possibly ambipolar (electron and hole) transport. We summarize the primary findings here as they illustrate many of the important issues in organic semiconductor design.

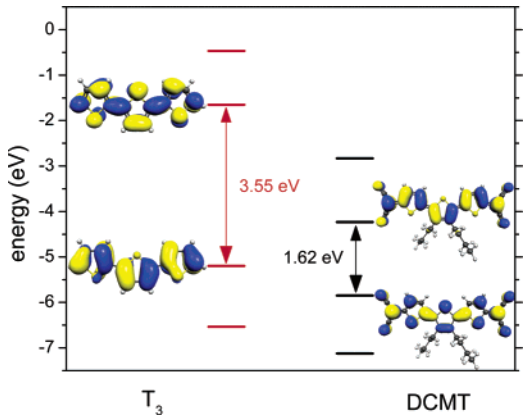


**Figure 10.** Upper two occupied and lower two unoccupied molecular orbitals of DCMT and $T_3$ calculated at the B3LYP/6-31G(d,p) level and shape of the LUMO (top) and HOMO (bottom) of DCMT and terthiophene ($T_3$) calculated at the same level. The energy shift of both the occupied and unoccupied orbitals of DCMT illustrate the stabilizing effect of the strongly electron withdrawing dicyanomethylene units.

**6.1. Molecular Properties.** *6.1.1. Electronic Structure.* Essentially, DCMT can be viewed as an oligothiophene dication stabilized by negatively charged dicyanomethyl termini. One-electron reduction of the quinoidal DCMT produces a radical *anion* which has the same resonance structure as the radical *cation* formed in well-studied aromatic oligothiophene materials.[89] For neutral DCMT, the degree of charge transfer from the thiophene core to the dicyanomethylene units has been estimated to be 0.4 electron from the IR $\nu$(C≡N) stretch, confirming the electron-withdrawing effects of the dicyanomethylene groups.[88]

The effect of the strongly electron withdrawing dicyanomethylene units on the electronic structure of DCMT is made clear in Figure 10, which shows the highest two occupied orbitals (HOMO and HOMO − 1) and the lowest two unoccupied orbitals (LUMO and LUMO + 1) for unsubstituted terthiophene ($T_3$) and DCMT (calculated on the basis of geometries optimized at the DFT/B3LYP level[90] with a 6-31G(d,p) basis set). The LUMO in DCMT is significantly stabilized compared to the LUMO in $T_3$. The calculated vertical electron affinity evolves from −0.17 eV in $T_3$ to −3.09 eV for DCMT, an increase of nearly 3 eV. The vertical ionization potential evolves to a much smaller extent, 0.24 eV, from 6.70 eV in $T_3$ to 6.94 eV for DCMT. In addition, the HOMO−LUMO energy difference decreases from 3.55 to 1.65 eV, which is a direct result of the quinoidal bonding in DCMT.

*6.1.2. Electrochemistry.* In contrast to p-channel materials, which should be easy to oxidize, n-channel materials should be easy to reduce; any candidate for an ambipolar material should be capable of both. The combination of an easily oxidized oligothiophene core with easily reduced dicyanomethylene groups in one $\pi$-system should show facile oxidations and reductions,

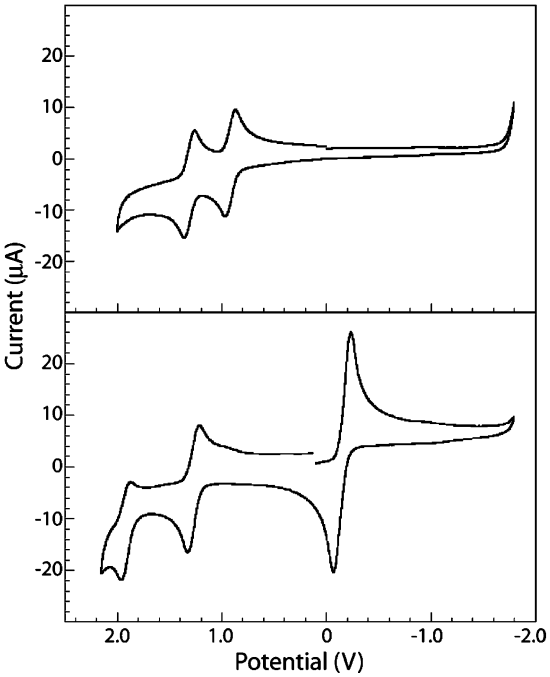


**Figure 11.** Cyclic voltammograms of an aromatic terthiophene (3,4′-di-*n*-butyl-5,5″-diphenyl-2,2′:5′,2″-terthiophene, top) and the quinoidal analogue DCMT (bottom). Scans are initiated in the negative direction from 0.0 V vs a saturated calomel reference electrode; cathodic currents are positive.

shown in Figure 11. Cyclic voltammograms of DCMT exhibit a reversible one-electron oxidation process with $E_0' = 1.27$ V, characterized by the appearance of an intense optical absorption at 688 nm in spectroelectrochemical studies, followed by a less reversible second oxidation at $E_{pa} = 1.96$.[86] The electron-accepting character of previously studied quinoid derivatives with one or two thiophene rings shows two discreet one-electron reductions. DCMT shows a two-electron reduction at $E_0' = -0.15$ V.[91]

**6.2. Solid-State Properties.** *6.2.1. Crystal Structure.* The single-crystal structure of DCMT (shown in Figure 12; $P2_1/c$, $a = 16.42$ Å, $b = 7.55$ Å, $c = 21.17$ Å, $\beta = 111.37°$) reveals a trans-coplanar orientation of thiophene rings. The quinoidal nature of this molecule is highlighted by alternating carbon−carbon double and single bonds, *in reverse* of the pattern observed in aromatic systems. Interannular $\pi$-bonds impose a planar structure on the atoms directly involved in the $\pi$-system. Molecules pack along the *b*-axis in dimer pairs 3.47 Å apart, which in turn $\pi$-stack at 3.63 Å distance and are slipped lengthwise by about one thiophene ring. In addition, DCMT packs with the alternating $\pi$-stacked columns tilted (viewed down the *a*-axis) at an angle of 39.4° from each other.[27,86]

*6.2.2. Thin Film Structure and Characterization.* DCMT can be vacuum sublimed at 130 °C to make highly crystalline thin films on $SiO_2$/Si substrates. Study by atomic force microscopy (AFM) reveals the grains of DCMT are terraced islands with lateral dimensions up to 10 $\mu$m and step heights of 17−19 Å, Figure 13b. The thin film XRD pattern, Figure 13a, reveals a 17.8 Å *d* spacing that is different from any line in the bulk powder pattern[28] and is greater than the long dimension of a DCMT molecule (16.2 Å); thus, the terraces do not simply correlate with the growth of the bulk crystalline

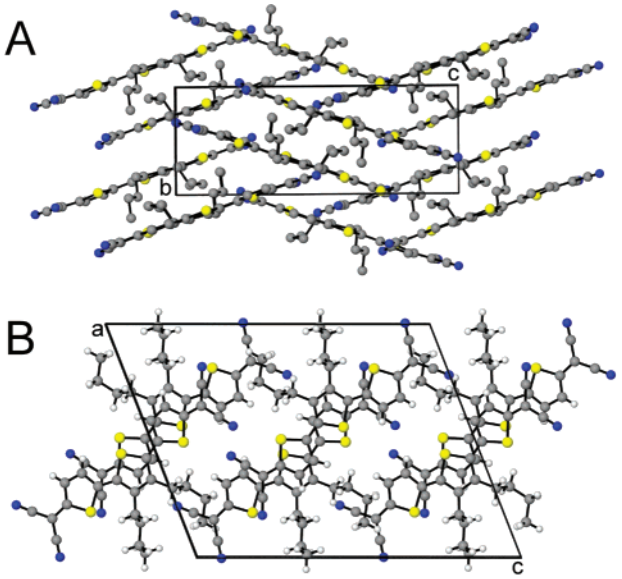


**Figure 12.** Views of the DCMT packing structure along the *a* axis (A) and the *b* axis (B).

phase or with homogeneous monolayers of molecules. The terraces have been modeled as $\pi$-dimerized DCMT molecules, tilted 39.4° with respect to the surface plane, and associated in extended stacks. Thus, analysis of the XRD data reveals that the DCMT molecules are arranged in the grains such that the $\pi$-stacking direction is parallel to the dielectric substrate, which is a favorable geometry for transport in OTFTs.

Replacement of the butyl groups on DCMT with −H gives a material with nearly identical molecular properties, but which grows needle-shaped grains rather than the platelike morphology, as can be seen in the SEM micrograph in Figure 13c. Films of this material are electrically inactive presumably because of poor grain−grain contact, illustrating that detailed structure−transport studies are often complicated by the tremendous sensitivity of film growth on every aspect of molecular structure.

**6.3. OTFT Devices.** OTFTs based on DCMT films grown on $SiO_2$/Si are made by evaporating Au or Ag source and drain contacts through a shadow mask. Figure 14 shows representative $I_D-V_D$ and $I_D-V_G$ characteristics for a high-mobility n-channel OTFT based on DCMT. Positive gate voltages turn the device on, indicating the charge carriers are electrons. The saturation electron mobility is 0.2 $cm^2\ V^{-1}\ s^{-1}$, a high value for electron transport, and the threshold voltage $V_T$ is +11 V. Devices generally exhibit an onset voltage $V_0$ of −15 V (shown in Figure 14b), an on-to-off current ratio $I_{ON}/I_{OFF}$ of $>10^6$, and a subthreshold swing *S* of 4.7 V $decade^{-1}$ of current.

The mobility and on-to-off current ratio are among the best reported for an n-channel material and are within an order of magnitude of those of pentacene. However, the subthreshold swing, which is a measure of how sharply the device transitions from off to on, is undesirably large. Large subthreshold swings are explained conventionally by the presence of traps at the insulator/semiconductor interface (interface states).[92]

DCMT films grown at elevated substrate temperatures (>136 °C), give a different morphology with greatly reduced n-channel mobility. However, there is

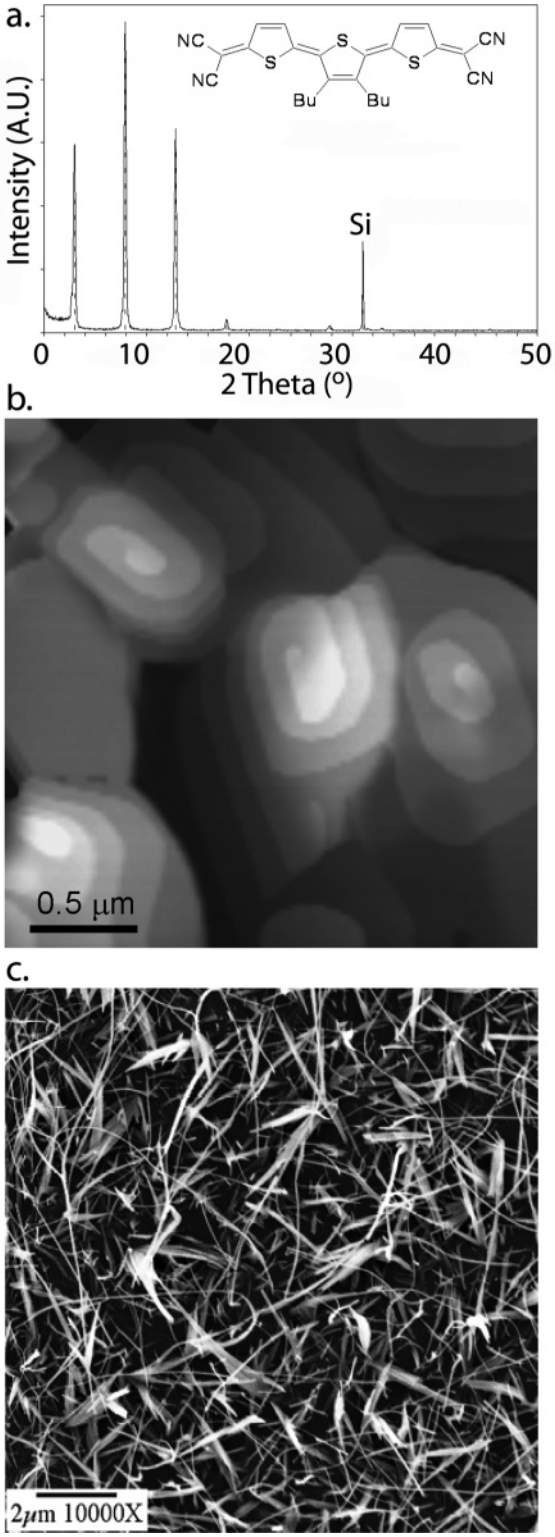


**Figure 13.** (a) X-ray diffraction of a 50 nm DCMT film on $SiO_2$. The inset shows the structure of DCMT. (b) AFM topograph of a DCMT film showing layered grain growth and screw dislocation growth of individual grains. (c) SEM micrograph of the needlelike morphology of "butyl-less" DCMT.

a surprising increase in current at large negative gate voltages, indicative of p-channel conduction. These devices turn on for both positive and negative gate voltages, with a narrow off region centered just negative of 0 V. Both the hole and electron mobilities in these devices are less than $10^{-4}$ cm$^2$ V$^{-1}$ s$^{-1}$.[28] To the best of our knowledge, this is one of only two examples of

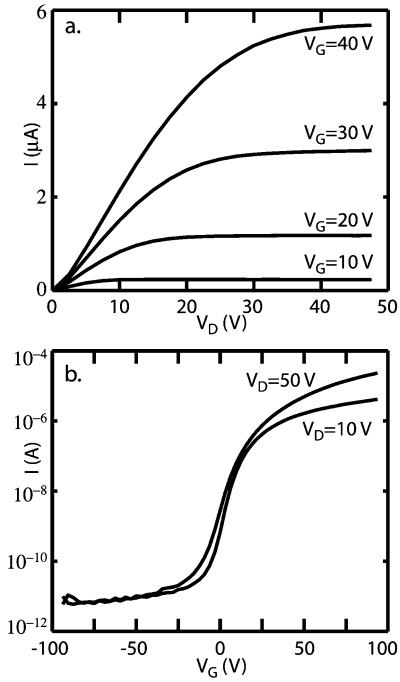


**Figure 14.** (a) $I_D-V_D$ characteristics for a high n-channel mobility DCMT TFT ($p^+$-Si/$SiO_2$ (300 nm)/DCMT (50 nm) with Au contacts). (b) $I_D-V_G$ characteristics of the same device. Using the saturation model to calculate FET parameters, $\mu_{FET}$ = 0.18 cm$^2$ V$^{-1}$ s$^{-1}$, $V_0$ = −15 V, $V_T$ = +11 V, $I_{ON}/I_{OFF} > 10^6$, and $S$ = 4.7 V decade$^{-1}$.

ambipolar transport in a TFT based on a single conjugated organic semiconductor material. Thus, the transport results are consistent with the electronic structure calculations and solution characterization of DCMT, which indicated the molecule could be reduced and had a crystal structure suitable for transport. More work needs to be done to understand trapping in DCMT OTFTs and the effects of environmental exposure, since transistor performance degrades upon exposure to air.

## 7. Future Directions

A specific challenge to materials chemists is to design solution-processable, air-stable organic semiconductors (p- or n-channel) that have significantly *better* performance in TFTs than amorphous silicon (a-Si). For example, achieving a charge mobility near 10 cm$^2$ V$^{-1}$ s$^{-1}$ (a factor of 10 better than that of a-Si) in an air-stable, solution-processed film, while maintaining low threshold voltages and high on-to-off current ratios, would significantly alter the competitive landscape for applications of organic semiconductors because the range of possible circuit designs increases as the mobility increases. Achieving this performance is a formidable challenge, and it is reasonable to question whether the performance limits of organic semiconductors have already been reached with current materials. However, understanding of structure−property relationships in organic semiconductors is essentially in its infancy, suggesting that with new knowledge significant improvements in transport properties will be possible. Indeed, recent exciting results for transistors based on organic semiconductor single crystals show that room temperature mobilities can be *higher* than 10 cm$^2$ V$^{-1}$ s$^{-1}$,[93] providing encouragement that future improve-

ments can be made in charge transport in organic semiconductor thin films.

Many basic structure−property issues in organic semiconductors are unclear and need to be addressed in future work. We do not, as yet, have a full understanding of the transport mechanism in OTFTs, and this is of course a major impediment to rational design of materials with improved transport behavior. Nor do we know the nature of the charge carrier traps in OTFTs. In the context of n-channel semiconductors, air stability and carrier trapping appear to be intricately related, and the roles of $O_2$ and $H_2O$ in trapping will need to be elucidated. Identifying trapping states will likely require the application of spectroscopy and scanning probe techniques to probe localized charge states in the ultrathin channel layer in OTFTs.

As emphasized in this review, there are significant opportunities for combining synthetic chemistry with electronic structure calculations and transport measurements to determine basic structure−transport relationships, which can serve as the basis for improved materials design. Questions that can be addressed systematically using this combination of methods include determination of what kind of crystal packing (e.g., herringbone versus $\pi$-stacking) is most favorable for transport and whether intermolecular electronic overlap can be enhanced by tuning the crystal packing (e.g., the degree of intermolecular ring slip) or by increasing the strength of intermolecular bonding. Surprisingly, very little has been done to exploit bonding other than the dispersive and quadrupolar interactions in the design of organic semiconductor solid-state structures. Whether directional H-bonding between semiconductor molecules can enhance carrier mobility, for example, remains an open question. Crystal engineering likely will play a prominent role in future organic semiconductor development.[94,95]

Thin film growth, both from the vapor phase and from solution, will continue to be a critical issue. The role of microstructure in transport is still under investigation, and only recently have grazing incidence X-ray scattering[96,97] and transmission electron microscopy[98] studies been performed to establish the molecular order at a few specific dielectric/semiconductor interfaces.

Finally, the issue of device stability, particularly for OTFTs based on n-channel materials, is emerging as perhaps the most crucial hurdle in the short term. Methods will need to be found to protect n-channel layers from the ambient or to decrease the semiconductor sensitivity to $O_2$ and $H_2O$ for the lifetime of the device (perhaps thousands of hours). In future OTFT development work it will become important to demonstrate performance in air and to report on the observable hysteresis in the $I-V$ characteristics as a function of device operating parameters. At the present, it appears that perfluorinated molecules such as $F_{16}CuPc$ and molecules with fluorinated end groups such as NTCDI-$CH_2C_6H_4CF_3$ offer the best combination of high mobility and air stability.

## 8. Conclusions

We have summarized the recent progress in the field of n-channel organic semiconductors and have outlined the properties that these materials must have to be incorporated into OTFTs. The important role of quantum calculations to understand the effects of chemical substituents and crystal packing on electronic structure was emphasized. The interplay of molecular properties and solid-state properties was highlighted by a case study of the development of a new n-channel semiconductor that has performance comparable to that of typical p-channel materials. Progress in the past five years has been substantial, but continued development of n-channel organic semiconductors will require a much better understanding of structure−property relationships than we currently have. A particularly important issue for n-channel materials is air stability. Significantly, closing the structure−property knowledge gap offers promising opportunities to improve the performance of n-channel organic semiconductors for OTFT applications.

**Acknowledgment.** Portions of the work described here were supported primarily by the MRSEC Program of the National Science Foundation under Award Number DMR-0212302. C.R.N. thanks the U.S. Army Research Office for an NDSEG Fellowship. D.A.d.S.F. and J.-L.B. thank the Minnesota Supercomputer Institute.

## References

(1) Bao, Z.; Rogers, J. A.; Katz, H. E. *J. Mater. Chem.* **1999**, *9*, 1895.
(2) Rogers, J. A.; Bao, Z.; Katz, H. E.; Dodabalapur, A. *Thin-Film Transistors* **2003**, 377.
(3) Dimitrakopoulos, C. D.; Malenfant, P. R. L. *Adv. Mater.* **2002**, *14*, 99.
(4) Katz, H. E.; Bao, Z. *J. Phys. Chem. B* **2000**, *104*, 671.
(5) Nelson, S. F.; Lin, Y. Y.; Gundlach, D. J.; Jackson, T. N. *Appl. Phys. Lett.* **1998**, *72*, 1854.
(6) Baude, P. F.; Ender, D. A.; Haase, M. A.; Kelley, T. W.; Muyres, D. V.; Theiss, S. D. *Appl. Phys. Lett.* **2003**, *82*, 3964.
(7) Gundlach, D. J.; Nichols, J. A.; Zhou, L.; Jackson, T. N. *Appl. Phys. Lett.* **2002**, *80*, 2925.
(8) Kymissis, I.; Dimitrakopoulos, C. D.; Purushothaman, S. *IEEE Trans. Electron Devices* **2001**, *48*, 1060.
(9) Neamen, D. A., Ed. *Semiconductor Physics and Devices: Basic Principles*, 2nd ed.; Irwin: Chicago, 1996.
(10) Chesterfield, R. J.; McKeen, J.; Newman, C. R.; Frisbie, C. D. *J. Appl. Phys.* **2004**, *95*, 6396.
(11) Hill, I. G.; Kahn, A. *Proc. SPIE* **1998**, *3476*, 168.
(12) Pope, M.; Swenberg, C. E. *Electronic Processes in Organic Crystals and Polymers*, 2nd ed.; Oxford University Press: New York, 1999.
(13) de Leeuw, D. M.; Simenon, M. M. J.; Brown, A. R.; Einerhand, R. E. F. *Synth. Met.* **1997**, *87*, 53.
(14) Guillaud, G.; Al Sadoun, M.; Maitrot, M.; Simon, J.; Bouvet, M. *Chem. Phys. Lett.* **1990**, *167*, 503.
(15) Brown, A. R.; de Leeuw, D. M.; Lous, E. J.; Havinga, E. E. *Synth. Met.* **1994**, *66*, 257.
(16) Laquindanum, J. G.; Katz, H. E.; Dodabalapur, A.; Lovinger, A. J. *J. Am. Chem. Soc.* **1996**, *118*, 11331.
(17) Bao, Z.; Lovinger, A. J.; Brown, J. *J. Am. Chem. Soc.* **1998**, *120*, 207.
(18) Haddon, R. C.; Perel, A. S.; Morris, R. C.; Palstra, T. T. M.; Hebard, A. F.; Fleming, R. M. *Appl. Phys. Lett.* **1995**, *67*, 121.
(19) Kobayashi, S.; Takenobu, T.; Mori, S.; Fujiwara, A.; Iwasa, Y. *Appl. Phys. Lett.* **2003**, *82*, 4581.
(20) Horowitz, G.; Delannoy, P. *Handb. Oligo- and Polythiophenes* **1999**, 283.
(21) Horowitz, G.; Hajlaoui, R.; Fichou, D.; El Kassmi, A. *J. Appl. Phys.* **1999**, *85*, 3202.
(22) Facchetti, A.; Deng, Y.; Wang, A.; Koide, Y.; Sirringhaus, H.; Marks, T. J.; Friend, R. H. *Angew. Chem., Int. Ed.* **2000**, *39*, 4547.
(23) Facchetti, A.; Mushrush, M.; Katz, H. E.; Marks, T. J. *Adv. Mater.* **2003**, *15*, 33.
(24) Facchetti, A.; Wang, A.; Marks, T. J. *Polym. Mater. Sci. Eng.* **2000**, *83*, 290.
(25) Facchetti, A.; Yoon, M.-h.; Katz, H. E.; Mushrush, M.; Marks, T. J. *Mater. Res. Soc. Symp. Proc.* **2003**, *769*, 375.
(26) Facchetti, A.; Yoon, M.-H.; Stern, C. L.; Katz, H. E.; Marks, T. J. *Angew. Chem., Int. Ed.* **2003**, *42*, 3900.

(27) Pappenfus, T. M.; Chesterfield, R. J.; Frisbie, C. D.; Mann, K. R.; Casado, J.; Raff, J. D.; Miller, L. L. *J. Am. Chem. Soc.* **2002**, *124*, 4184.
(28) Chesterfield, R. J.; Newman, C. R.; Pappenfus, T. M.; Ewbank, P. C.; Haukaas, M. H.; Mann, K. R.; Miller, L. L.; Frisbie, C. D. *Adv. Mater.* **2003**, *15*, 1278.
(29) Meijer, E. J.; De Leeuw, D. M.; Setayesh, S.; van Veenendaal, E.; Huisman, B. H.; Blom, P. W. M.; Hummelen, J. C.; Scherf, U.; Klapwijk, T. M. *Nat. Mater.* **2003**, *2*, 678.
(30) Waldauf, C.; Schilinsky, P.; Perisutti, M.; Hauch, J.; Brabec, C. J. *Adv. Mater.* **2003**, *15*, 2084.
(31) Ostrick, J. R.; Dodabalapur, A.; Torsi, L.; Lovinger, A. J.; Kwock, E. W.; Miller, T. M.; Galvin, M.; Berggren, M.; Katz, H. E. *J. Appl. Phys.* **1997**, *81*, 6804.
(32) Katz, H. E.; Johnson, J.; Lovinger, A. J.; Li, W. *J. Am. Chem. Soc.* **2000**, *122*, 7787.
(33) Malenfant, P. R. L.; Dimitrakopoulos, C. D.; Gelorme, J. D.; Kosbar, L. L.; Graham, T. O.; Curioni, A.; Andreoni, W. *Appl. Phys. Lett.* **2002**, *80*, 2517.
(34) Chesterfield, R. J.; McKeen, J.; Newman, C. R.; Ewbank, P. C.; Frisbie, C. D. *J. Phys. Chem. B*, submitted for publication.
(35) Babel, A.; Jenekhe, S. A. *Adv. Mater.* **2002**, *14*, 371.
(36) Babel, A.; Jenekhe, S. A. *J. Am. Chem. Soc.* **2003**, *125*, 13656.
(37) Chen, Z.; Debije, M. G.; Debaerdemaeker, T.; Osswald, P.; Wuerthner, F. *ChemPhysChem* **2004**, *5*, 137.
(38) Meng, H.; Chen, Y.; Wudl, F. *Macromolecules* **2001**, *34*, 5071.
(39) Tonzola, C. J.; Alam, M. M.; Kaminsky, W.; Jenekhe, S. A. *J. Am. Chem. Soc.* **2003**, *125*, 13548.
(40) Zhu, Y.; Alam, M. M.; Jenekhe, S. A. *Macromolecules* **2003**, *36*, 8958.
(41) Yassar, A.; Demanze, F.; Fichou, D. *Opt. Mater. (Amsterdam)* **1999**, *12*, 379.
(42) Yassar, A.; Demanze, F.; Jaafari, A.; El Idrissi, M.; Coupry, C. *Adv. Funct. Mater.* **2002**, *12*, 699.
(43) Sakamoto, Y.; Suzuki, T.; Miura, A.; Fujikawa, H.; Tokito, S.; Taga, Y. *J. Am. Chem. Soc.* **2000**, *122*, 1832.
(44) Sakamoto, Y.; Komatsu, S.; Suzuki, T. *J. Am. Chem. Soc.* **2001**, *123*, 4643.
(45) Liu, S.-G.; Sui, G.; Cormier, R. A.; Leblanc, R. M.; Gregg, B. A. *J. Phys. Chem. B* **2002**, *106*, 1307.
(46) Pappenfus, T. M.; Burand, M. W.; Janzen, D. E.; Mann, K. R. *Org. Lett.* **2003**, *5*, 1535.
(47) Heidenhain, S. B.; Sakamoto, Y.; Suzuki, T.; Miura, A.; Fujikawa, H.; Mori, T.; Tokito, S.; Taga, Y. *J. Am. Chem. Soc.* **2000**, *122*, 10240.
(48) McKeen, J.; Newman, C. R.; Frisbie, C. D. Unpublished results.
(49) Facchetti, A.; Marks, T. J. Personal communication.
(50) Horowitz, G. *Adv. Mater.* **1998**, *10*, 365.
(51) Bredas, J. L.; Calbert, J. P.; Da Silva Filho, D. A.; Cornil, J. *Proc. Natl. Acad. Sci. U.S.A.* **2002**, *99*, 5804.
(52) Desiraju, G. R.; Gavezzotti, A. *J. Chem. Soc., Chem. Commun.* **1989**, 621.
(53) Desiraju, G. R.; Gavezzotti, A. *Acta Crystallogr., Sect. B: Struct. Sci.* **1989**, *B45*, 473.
(54) Kline, R. J.; McGehee, M. D.; Kadnikova, E. N.; Liu, J.; Frechet, J. M. J. *Adv. Mater.* **2003**, *15*, 1519.
(55) Matters, M.; De Leeuw, D. M.; Herwig, P. T.; Brown, A. R. *Synth. Met.* **1999**, *102*, 998.
(56) Volkel, A. R.; Street, R. A.; Knipp, D. *Phys. Rev. B* **2002**, *66*, 195336/1.
(57) Sirringhaus, H.; Kawase, T.; Friend, R. H.; Shimoda, T.; Inbasekaran, M.; Wu, W.; Woo, E. P. *Science* **2000**, *290*, 2123.
(58) Afzali, A.; Dimitrakopoulos, C. D.; Breen, T. L. *J. Am. Chem. Soc.* **2002**, *124*, 8812.
(59) Brown, A. R.; Jarrett, C. P.; de Leeuw, D. M.; Matters, M. *Synth. Met.* **1997**, *88*, 37.
(60) Bredas, J.-L.; Cornil, J.; Beljonne, D.; Dos Santos, D. A.; Shuai, Z. *Acc. Chem. Res.* **1999**, *32*, 267.
(61) Klauk, H.; Schmid, G.; Radlik, W.; Weber, W.; Zhou, L.; Sheraw, C. D.; Nichols, J. A.; Jackson, T. N. *Solid-State Electron.* **2002**, *47*, 297.
(62) Burgi, L.; Richards, T. J.; Friend, R. H.; Sirringhaus, H. *J. Appl. Phys.* **2003**, *94*, 6129.
(63) Street, R. A.; Salleo, A. *Appl. Phys. Lett.* **2002**, *81*, 2887.
(64) Klauk, H.; Jackson, T. N. *Mol. Nanoelectron.* **2003**, 291.
(65) Necliudov, P. V.; Shur, M. S.; Gundlach, D. J.; Jackson, T. N. *Solid-State Electron.* **2002**, *47*, 259.
(66) Bredas, J. L.; Street, G. B. *Acc. Chem. Res.* **1985**, *18*, 309.
(67) Su, W. P.; Schrieffer, J. R.; Heeger, A. J. *Phys. Rev. Lett.* **1979**, *42*, 1698.
(68) Duke, C. B.; Schein, L. B. *Phys. Today* **1980**, *33*, 42.
(69) Marcus, R. A. *Rev. Mod. Phys.* **1993**, *65*, 599.
(70) Silbey, R.; Jortner, J.; Rice, S. A.; Vala, M. T., Jr. *J. Chem. Phys.* **1965**, *42*, 733.
(71) Barbara, P. F.; Meyer, T. J.; Ratner, M. A. *J. Phys. Chem.* **1996**, *100*, 13148.
(72) Balzani, V.; Juris, A.; Venturi, M.; Campagna, S.; Serroni, S. *Chem. Rev.* **1996**, *96*, 759.
(73) Cornil, J.; Calbert, J. P.; Bredas, J. L. *J. Am. Chem. Soc.* **2001**, *123*, 1250.
(74) Malagoli, M.; Bredas, J. L. *Chem. Phys. Lett.* **2000**, *327*, 13.
(75) Cornil, J.; Beljonne, D.; Calbert, J.-P.; Bredas, J.-L. *Adv. Mater.* **2001**, *13*, 1053.
(76) Li, X.-Y.; Tang, X.-S.; He, F.-C. *Chem. Phys.* **1999**, *248*, 137.
(77) Cornil, J.; Calbert, J. P.; Beljonne, D.; Silbey, R.; Bredas, J. L. *Synth. Met.* **2001**, *119*, 1.
(78) Frisch, M. J.; et. al. *Gaussian 98*, revision A11; Gaussian, Inc.: Pittsburgh, PA, 1998.
(79) Cornil, J.; Dos Santos, D. A.; Beljonne, D.; Bredas, J. L. *J. Phys. Chem.* **1995**, *99*, 5604.
(80) Bredas, J. L.; Heeger, A. J. *Chem. Phys. Lett.* **1994**, *217*, 507.
(81) Klebe, G.; Graser, F.; Haedicke, E.; Berndt, J. *Acta Crystallogr., Sect. B: Struct. Sci.* **1989**, *B45*, 69.
(82) Kazmaier, P. M.; Hoffmann, R. *J. Am. Chem. Soc.* **1994**, *116*, 9684.
(83) Haedicke, E.; Graser, F. *Acta Crystallogr., Sect. C: Cryst. Struct. Commun.* **1986**, *C42*, 189.
(84) Zerner, M. C.; Loew, G. H.; Kirchner, R. F.; Mueller-Westerhoff, U. T. *J. Am. Chem. Soc.* **1980**, *102*, 589.
(85) Ridley, J.; Zerner, M. *Theor. Chim. Acta* **1973**, *32*, 111.
(86) Pappenfus, T. M.; Raff, J. D.; Hukkanen, E. J.; Burney, J. R.; Casado, J.; Drew, S. M.; Miller, L. L.; Mann, K. R. *J. Org. Chem.* **2002**, *67*, 6015.
(87) Casado, J.; Miller, L. L.; Mann, K. R.; Pappenfus, T. M.; Higuchi, H.; Orti, E.; Milian, B.; Pou-Amerigo, R.; Hernandez, V.; Lopez Navarrete, J. T. *J. Am. Chem. Soc.* **2002**, *124*, 12380.
(88) Casado, J.; Pappenfus, T. M.; Mann, K. R.; Milian, B.; Orti, E.; Viruela, P. M.; Ruiz Delgado, M. C.; Hernandez, V.; Lopez Navarrete, J. T. *J. Mol. Struct.* **2003**, *651−653*, 665.
(89) Graf, D. D.; Duan, R. G.; Campbell, J. P.; Miller, L. L.; Mann, K. R. *J. Am. Chem. Soc.* **1997**, *119*, 5888.
(90) Frisch, M. J.; et. al.; *Gaussian 03*, revision B01; Gaussian, Inc.: Pittsburgh, PA, 2003.
(91) Higuchi, H.; Nakayama, T.; Koyama, H.; Ojima, J.; Wada, T.; Sasabe, H. *Bull. Chem. Soc. Jpn.* **1995**, *68*, 2363.
(92) Sze, S. M. *Physics of Semiconductor Devices*, 2nd ed.; Wiley-Interscience: New York, 1999.
(93) Sundar, V. C.; Zaumseil, J.; Podzorov, V.; Menard, E.; Willett, R. L.; Someya, T.; Gershenson, M. E.; Rogers, J. A. *Science* **2004**, *303*, 1644.
(94) Curtis, M. D.; Cao, J.; Kampf, J. W. *J. Am. Chem. Soc.* **2004**, *126*, 4318.
(95) Desiraju, G. R. *J. Mol. Struct.* **2003**, *656*, 5.
(96) Fritz, S. E.; Martin, S. M.; Frisbie, C. D.; Ward, M. D.; Toney, M. F. *J. Am. Chem. Soc.* **2004**, *126*, 4084.
(97) Malliaras, G. G. Personal communication.
(98) Drummy, L. F.; Kubel, C.; Lee, D.; White, A.; Martin, D. C. *Adv. Mater.* **2002**, *14*, 54.

CM049391X